Materials and Design 94 (2016) 546–553

Contents lists available at ScienceDirect

Materials and Design

journal homepage: www.elsevier.com/locate/matdes

Numerical estimation of effective electromagnetic properties for design of particulate composites

Bhavesh Patel *, Tarek I. Zohdi

Department of Mechanical Engineering, University of California, Berkeley, CA 94720, United States

ARTICLE INFO

Article history:
Received 25 October 2015
Received in revised form 26 October 2015
Accepted 5 January 2016
Available online 12 January 2016

Keywords:
Electrical properties
Magnetic properties
Computational modeling
Composites design

ABSTRACT

Most modern electromagnetic devices consist of dielectric and magnetic particulate composites. Predicting the effective electric permittivity and effective magnetic permeability of the envisioned composite is of great importance in validating the design for such applications. In this work, we propose a numerical method based on Yee's scheme and statistically generated representative volume element to estimate these effective electromagnetic properties for linear isotropic composites made with ellipsoidal particles. By considering particle geometry and composite microstructure precisely, it provides a more accurate tool for their design than available analytical bounds. Several numerical examples of composite microstructures are presented to demonstrate the capability of the proposed method. Comparison with analytical bounds and experimental results from literature is conducted to show validity.

© 2016 Elsevier Ltd. All rights reserved.

1. Introduction

Dielectric and magnetic particulate composites have become the primary choice for manufacturing electromagnetic devices [1,2] due to the potential they offer in tailoring a material with desired properties [3,4]. Dielectric insulators for capacitors [5,6] and magnetic cores for inductors [7] are two examples where interest in such composites has recently risen, driven by the requirement for higher performance to achieve further miniaturization. Particles with characteristic length ranging from *nm* to *μm* are generally sought for preparing a composite material in the *μm* to *mm* range.

Average properties obtained by homogenization, called effective properties [8], have been introduced for better characterization of the macroscopic response of such composites. For the electromagnetic (EM) applications mentioned previously, estimating the effective electric permittivity ϵ^* (in F/m) and the effective magnetic permeability μ^* (in H/m), is of prime importance to predict the behavior of the composite and assess the success of its design for a desired application. For a linear isotropic composite, these effective properties are defined as follows [9]

$$\langle \mathbf{D} \rangle_\Omega = \epsilon^* \langle \mathbf{E} \rangle_\Omega \tag{1}$$

$$\langle \mathbf{B} \rangle_\Omega = \mu^* \langle \mathbf{H} \rangle_\Omega \tag{2}$$

where Ω refers to the volume of the composite material, $\langle \mathbf{D} \rangle_\Omega$ represents the average electric flux density over Ω (in C/m^2), $\langle \mathbf{E} \rangle_\Omega$ is the average electric field intensity over Ω (in V/m), $\langle \mathbf{B} \rangle_\Omega$ gives the average magnetic flux density over Ω (in T), and $\langle \mathbf{H} \rangle_\Omega$ refers to the average magnetic field intensity over Ω (in A/m). The averaging operator $\langle \cdot \rangle_\Omega$ applies to each component of a vector field, and is defined for the ith component of any vector $\mathbf{G}$ as $\langle G_i \rangle_\Omega = \frac{1}{|\Omega|}\int_\Omega G_i \mathrm{d}\Omega$. Taking the dot product of the left and right hand sides in Eqs. (1) and (2) leads to the explicit formulation

$$\epsilon^* = \sqrt{\frac{\langle \mathbf{D} \rangle_\Omega \cdot \langle \mathbf{D} \rangle_\Omega}{\langle \mathbf{E} \rangle_\Omega \cdot \langle \mathbf{E} \rangle_\Omega}} \tag{3}$$

$$\mu^* = \sqrt{\frac{\langle \mathbf{B} \rangle_\Omega \cdot \langle \mathbf{B} \rangle_\Omega}{\langle \mathbf{H} \rangle_\Omega \cdot \langle \mathbf{H} \rangle_\Omega}} \tag{4}$$

Relative effective properties $\epsilon_r^* = \frac{\epsilon^*}{\epsilon_0}$ and $\mu_r^* = \frac{\mu^*}{\mu_0}$ are commonly used, where ϵ_0 and μ_0 are the permittivity and the permeability constants of free space, respectively. Direct evaluations of ϵ^* and μ^* using formulations 3 and 4 are not possible due to the complexities involved in evaluating the average EM fields over a composite. Several analytical formulas have been derived in the past, that provide upper and lower bounds to these effective properties values given the EM properties and volume fractions of the constituents in the composite. We can cite the widely used Wiener bounds [10] and Hashin–Shtrikman bounds [11] — the lower Hashin bound is popularly known as the Maxwell–Garnett approximation [12]. They are commonly used for first hand estimation during design, before

* Corresponding author.
E-mail addresses: b.patel@berkeley.edu (B. Patel), zodhi@berkeley.edu (T.I. Zohdi).

http://dx.doi.org/10.1016/j.matdes.2016.01.015
0264-1275/© 2016 Elsevier Ltd. All rights reserved.

conducting experimental validation. The accuracy of these bounds is however limited because they provide a range that increases significantly as the differences in the value of the properties between the constituents increase. Numerical methods were initially developed to estimate effective mechanical properties [13,14]. Extensions for effective EM properties were introduced in [9] for spherical particle-reinforced composites.

In the present study, we develop a numerical framework to estimate the effective EM properties ϵ^* and μ^* for any given linear isotropic particulate composite. Following [9,14], it consists of building a numerical sample of the composite material of interest, and applying EM field at its interface. Then, Maxwell's equations [15] are solved numerically over the sample to obtain its EM response and subsequently compute the effective EM properties. The novelty resides in the use of Yee's scheme [16], a Finite Difference Time Domain (FDTD) scheme specifically designed for Maxwell's equations. Moreover, this method is designed to handle composites with multiple phases consisting of a matrix material and multiple types of ellipsoidal particles. Illustration of such composite is presented in Fig. 1. Additionally, parallel implementation of the numerical solver is done for high computational performance, allowing material designer to conduct simulation on a single computer without requiring exceptional computational power. Precise consideration of the particles geometry in 3D allows for a more accurate estimation than the analytical bounds mentioned previously. Also, consideration of dynamic Maxwell's equations provides enough flexibility to further envision effect of external dynamic phenomena. For instance temperature rise could be significant in the applications of interest due to Joule's effect, and it has been shown to have considerable effect on the EM properties of certain thermo-sensible materials [17,18,19]. This could be taken into account by solving energy conservation equation simultaneously with Maxwell's equations, using for instance a staggered scheme for coupled physics as in [20]. Thus, this method is intended to set a basis for the multiphysics design of particulate composite intended for EM applications. A possibility that is not offered by the analytical bounds.

The organization of this paper is as follows. In Section 2, the proposed numerical method to compute the effective EM properties of particulate composites is presented. Application to model problems is realized in Section 3 to validate the method using analytical bounds and experimental results found in literature. Concluding remarks are finally drawn in Section 4. Throughout the study, we neglect thermal, stress, strain, and chemical effects. Constituents and resulting composites are assumed to be linear, isotropic, and non-dispersive. We consider the particles to be non-overlapping and having hard shell interface.

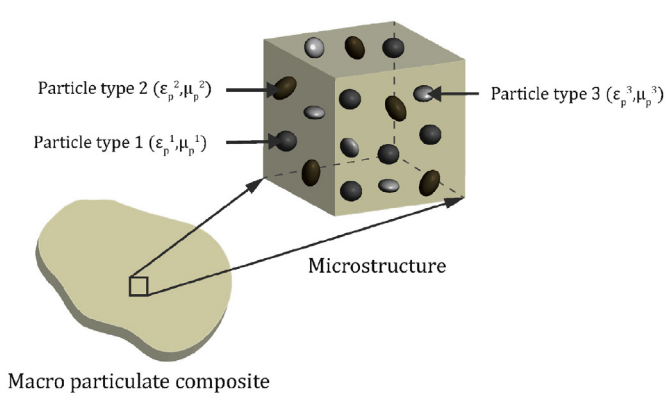

Fig. 1. Illustration of the homogenization process for a 4 phases composite made with $Q=3$ types of particles.

2. Numerical method

2.1. Representative volume element

Solving Maxwell's equations using any numerical technique would require meshing of the composite of interest. To capture the particles into the numerical scheme, and take the microstructure of the composite properly into account, a fine enough mesh would be required. Usually, a mesh size of a tenth of the characteristic length of a particle is prescribed — this is verified during application to model problems in the next section. Due to the scale difference between the overall composite size and the particle size in our problem, this would result in an enormous amount of unknowns to solve for. For instance, for a cubic composite of side $1mm$ filled with particles of diameter $1\mu m$, a mesh of $0.1\mu m$ would be adequate, resulting in 10^4 nodes in each direction and a total number of 10^{12} nodes. This would obviously be too heavy for efficient computations — a reasonable amount for computation over a single computer is 10^6 nodes in total. To overcome this problem, commonly encountered while computing effective properties numerically, the notion of a representative volume element (RVE) has been introduced [21,22]. We declare L as the characteristic length of the actual composite, l as the characteristic length of the RVE, and d as the characteristic length of the particles. A schematic of the different scales involved is shown in Fig. 2.

Basically a RVE is a cubic piece, "taken" from the actual composite material, that is small enough ($l \ll L$) so that efficient computation could be carried out and estimated properties could be considered as material point properties, but big enough to properly represent the microstructure ($l \gg d$). Additionally, the volume fraction of all constituents must be similar to the actual composite for adequate representation. Also, the particles must be randomly distributed and oriented in order to simulate randomness and isotropy of the actual composite. In this work, the simple RVE generation algorithm known as Random Sequential Adsorption (RSA) [23], is employed. Based on the specified RVE size l, the number of particle N_p^q required to satisfy the desired volume fraction v_p^q is computed for each type of particles q. Then, all particles are added to the RVE cube one by one by generating random position $(x_1^{q,r}, x_2^{q,r}, x_3^{q,r})$ for the center of gravity and random orientation $(\alpha_1^{q,r}, \alpha_2^{q,r}, \alpha_3^{q,r})$ for the principle axis of the rth particle of q type. For each new particle, a check is performed to determine if overlapping occurs with any of the previously added particles using the method from [24], that basically consist of verifying if two ellipsoids share any common volume. If overlapping occurs, the position and orientation are rejected, and the process is repeated. The complete process is described in Algorithm 1, and the parameters used are illustrated in Fig. 3. We notice that this simple RVE generating algorithm limit the total volume fraction of particles to about 0.2 that is sufficient for most common composites. To incorporate studies of composites with higher particle volume fraction, advanced RVE generator algorithm could be used, as the ones described in [25]. In such algorithm, the particles are not placed randomly in the entire RVE volume but rather into restricted volume, or cell, in order to use

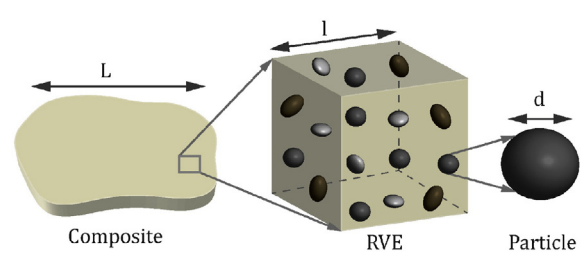

Fig. 2. Illustration of the different scales involved in RVE size estimation.

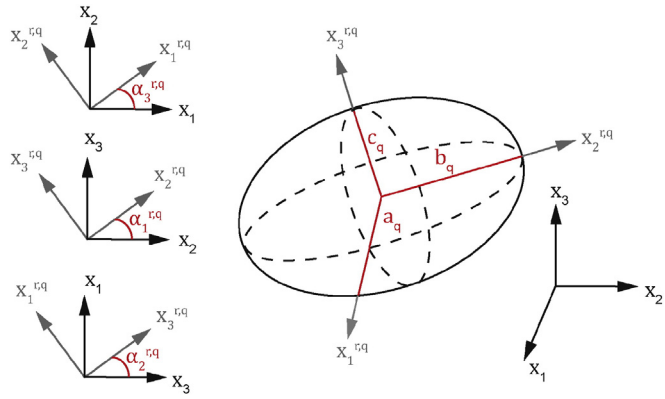

Fig. 3. Illustration of the parameters used to describe the rth ellipsoidal particle of type q.

available volume optimally and incorporate larger amount of non-overlapping particles.

The conditions mentioned previously provide only vague indications on the size of the RVE, without giving quantitative dimensions. The usual technique is to start with an arbitrary initial size l that satisfies previously mentioned qualitative requirements, estimate effective properties over it, then increase the size by a controlled value Δl and repeat until variation of results is less than a specified tolerance tol_S. For each RVE size l during the size estimation process, computation of effective properties over several RVEs is necessary to obtain statistically significative results. The average effective properties over all RVEs are then considered for size convergence analysis. No actual condition is prescribed on the number M of RVEs. The greater it is, the better randomness of the particle repartition in the actual composite would be taken into account. However, it has to be limited based on available computational power to ensure efficiency of the method. Evaluation over each RVE is an independent process that is parallelized in the proposed method for improved performance. Computation over up to M_c number of RVEs is conducted simultaneously, where M_c would be set based on the number of cores and processors available.

Algorithm 1. RVE generator.

Input : l, Q, (a_q, b_q, c_q) and v_p^q for each particle of type q
Output: $(x_1^{q,r}, x_2^{q,r}, x_3^{q,r})$ and $(\alpha_1^{q,r}, \alpha_2^{q,r}, \alpha_3^{q,r})$ for each particles

```
while q ≤ Q do
    l_m = max(a_q, b_q, c_q); Ω_p^q = (1/3)πa_q b_q c_q; N_p^q = |v_p^q l^3 / Ω_p^q|; r = 0;
    while r ≤ N_p^q do
        (x_s^{q,r}) = l_m + (l − l_m) * rand_s, 0 ≤ rand_s ≤ 1, s = 1,3 ;
        (α_s^{q,r}) = 2π * rand_s, 0 ≤ rand_s ≤ 1, s = 1,3 ;
        check overlapping with previous particles using method from [24];
        if overlap = false then
            save particle coordinates and orientation;
            r = r + 1;
        end
    end
    q=q+1;
end
```

2.2. Maxwell's equations

Let Ω be the total volume of the RVE that is considered, Ω_m the volume of the matrix material, and Ω_p the total volume of all of the particles

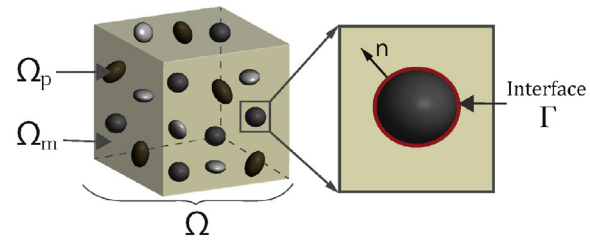

Fig. 4. Domain decomposition of a RVE.

in the RVE such that $\Omega = \Omega_m \cup \Omega_p$ (if there are Q types of particles, $\Omega_p = \sum_{q=1}^{Q} N_p^q \Omega_p^q$). Also, let's designate by Γ any particle/matrix interface. This is illustrated in Fig. 4. To compute the electromagnetic response of a RVE, the following system of local Maxwell's equations for linear isotropic materials [15,26,27] is to be solved over it to get the **E** and **H** fields in $\Omega_u (u = m or p)$:

$$\frac{\partial(\epsilon_u \mathbf{E})}{\partial t} + \sigma_u \mathbf{E} = \nabla \times \mathbf{H} \tag{5}$$

$$\frac{\partial(\mu_u \mathbf{H})}{\partial t} = -\nabla \times \mathbf{E} \tag{6}$$

on Γ:

$$\mathbf{n} \times (\mathbf{E}_m - \mathbf{E}_p) = 0 \tag{7}$$

$$\mathbf{n} \times (\mathbf{H}_m - \mathbf{H}_p) = 0 \tag{8}$$

$$\left((\epsilon E)_m - (\epsilon E)_p\right) \cdot \mathbf{n} = 0 \tag{9}$$

$$\left((\mu H)_m - (\mu H)_p\right) \cdot \mathbf{n} = 0 \tag{10}$$

where σ designates the electric conductivity (in S/m, it would be close to $0S/m$ for the applications of interest as we are focusing on dielectric materials but it is left here in the formulation for generalization), and the unit normal **n** at Γ is oriented from Ω_p to Ω_m (particle to matrix). Then, **D** and **B** fields are obtained using the constitutive laws for linear isotropic materials [28]

$$\mathbf{D} = \epsilon_u \mathbf{E} \tag{11}$$

$$\mathbf{B} = \mu_u \mathbf{H} \tag{12}$$

where $u = p$ if we are located inside a particle, or $u = m$ otherwise.

2.3. Yee's scheme

Yee's scheme [16] is implemented to solve the system of Eqs. (5) to (10) numerically. A meticulous explanation of this method and general computational electrodynamics discussions are available in [29,30]. This finite difference scheme uses a particular discretization where alternation in space and time occurs between the components of **E** and **H** in order to provide second order accuracy for both temporal and spatial computations. Additionally, it is fully explicit providing thus an efficient computational performance. The spatial discretization in 3D is made using the so-called Yee cell that is presented in Fig. 5. We call Δx_1, Δx_2, and Δx_3 the spatial discretization step size in direction $\mathbf{x}_1$, $\mathbf{x}_2$, and $\mathbf{x}_3$, respectively. Let Δt be the temporal discretization size. We introduce for any function $f(x_1, x_2, x_3, t)$ the notation $f_{i,j,k}^n = f(i\Delta x_1, j\Delta x_2, k\Delta x_3, n\Delta t)$. The following centered difference discretization of Eqs. (5) and (6) are

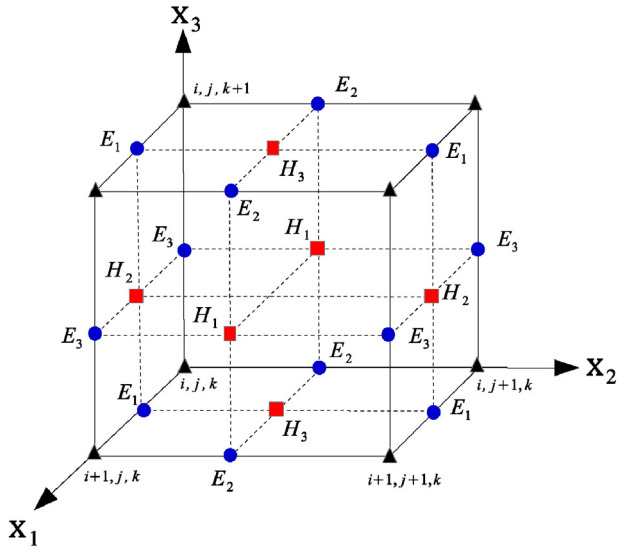

Fig. 5. Schematic of a Yee cell.

used in Yee's scheme

$$H_1|^{n+\frac{1}{2}}_{i,j+\frac{1}{2},k+\frac{1}{2}} = H_1|^{n}_{i,j+\frac{1}{2},k+\frac{1}{2}} + \frac{\Delta t}{\mu_{i,j+\frac{1}{2},k+\frac{1}{2}}}\left(\frac{E_2|^{n}_{i,j+\frac{1}{2},k+1} - E_2|^{n}_{i,j+\frac{1}{2},k}}{\Delta x_3} - \frac{E_3|^{n}_{i,j+1,k+\frac{1}{2}} - E_3|^{n}_{i,j,k+\frac{1}{2}}}{\Delta x_2}\right) \tag{13}$$

$$H_2|^{n+\frac{1}{2}}_{i+\frac{1}{2},j,k+\frac{1}{2}} = H_2|^{n}_{i+\frac{1}{2},j,k+\frac{1}{2}} + \frac{\Delta t}{\mu_{i+\frac{1}{2},j,k+\frac{1}{2}}}\left(\frac{E_3|^{n}_{i+1,j,k+\frac{1}{2}} - E_3|^{n}_{i,j,k+\frac{1}{2}}}{\Delta x_1} - \frac{E_1|^{n}_{i+\frac{1}{2},j,k+1} - E_1|^{n}_{i+\frac{1}{2},j,k}}{\Delta x_3}\right) \tag{14}$$

$$H_3|^{n+\frac{1}{2}}_{i+\frac{1}{2},j+\frac{1}{2},k} = H_3|^{n}_{i+\frac{1}{2},j+\frac{1}{2},k} + \frac{\Delta t}{\mu_{i+\frac{1}{2},j+\frac{1}{2},k}}\left(\frac{E_1|^{n}_{i+\frac{1}{2},j+1,k} - E_1|^{n}_{i+\frac{1}{2},j,k}}{\Delta x_2} - \frac{E_2|^{n}_{i+1,j+\frac{1}{2},k} - E_2|^{n}_{i,j+\frac{1}{2},k}}{\Delta x_1}\right) \tag{15}$$

$$E_1|^{n+1}_{i+\frac{1}{2},j,k} = \frac{2\epsilon_{i+\frac{1}{2},j,k} - \sigma_{i+\frac{1}{2},j,k}\Delta t}{2\epsilon_{i+\frac{1}{2},j,k} + \sigma_{i+\frac{1}{2},j,k}\Delta t}E_1|^{n}_{i+\frac{1}{2},j,k} + \frac{2\Delta t}{2\epsilon_{i+\frac{1}{2},j,k} + \sigma_{i+\frac{1}{2},j,k}\Delta t} \times\left(\frac{H_3|^{n+\frac{1}{2}}_{i+\frac{1}{2},j+\frac{1}{2},k} - H_3|^{n+\frac{1}{2}}_{i+\frac{1}{2},j-\frac{1}{2},k}}{\Delta x_2} - \frac{H_2|^{n+\frac{1}{2}}_{i+\frac{1}{2},j,k+\frac{1}{2}} - H_2|^{n+\frac{1}{2}}_{i+\frac{1}{2},j,k-\frac{1}{2}}}{\Delta x_3}\right) \tag{16}$$

$$E_2|^{n+1}_{i,j+\frac{1}{2},k} = \frac{2\epsilon_{i,j+\frac{1}{2},k} - \sigma_{i,j+\frac{1}{2},k}\Delta t}{2\epsilon_{i,j+\frac{1}{2},k} + \sigma_{i,j+\frac{1}{2},k}\Delta t}E_2|^{n}_{i,j+\frac{1}{2},k} + \frac{2\Delta t}{2\epsilon_{i,j+\frac{1}{2},k} + \sigma_{i,j+\frac{1}{2},k}\Delta t} \times\left(\frac{H_1|^{n+\frac{1}{2}}_{i,j+\frac{1}{2},k+\frac{1}{2}} - H_1|^{n+\frac{1}{2}}_{i,j+\frac{1}{2},k-\frac{1}{2}}}{\Delta x_3} - \frac{H_3|^{n+\frac{1}{2}}_{i+\frac{1}{2},j+\frac{1}{2},k} - H_3|^{n+\frac{1}{2}}_{i-\frac{1}{2},j+\frac{1}{2},k}}{\Delta x_1}\right) \tag{17}$$

$$E_3|^{n+1}_{i,j,k+\frac{1}{2}} = \frac{2\epsilon_{i,j,k+\frac{1}{2}} - \sigma_{i,j,k+\frac{1}{2}}\Delta t}{2\epsilon_{i,j,k+\frac{1}{2}} + \sigma_{i,j,k+\frac{1}{2}}\Delta t}E_3|^{n}_{i,j,k+\frac{1}{2}} + \frac{2\Delta t}{2\epsilon_{i,j,k+\frac{1}{2}} + \sigma_{i,j,k+\frac{1}{2}}\Delta t} \times\left(\frac{H_2|^{n+\frac{1}{2}}_{i+\frac{1}{2},j,k+\frac{1}{2}} - H_2|^{n+\frac{1}{2}}_{i-\frac{1}{2},j,k+\frac{1}{2}}}{\Delta x_1} - \frac{H_1|^{n+\frac{1}{2}}_{i,j+\frac{1}{2},k+\frac{1}{2}} - H_1|^{n+\frac{1}{2}}_{i,j-\frac{1}{2},k+\frac{1}{2}}}{\Delta x_2}\right) \tag{18}$$

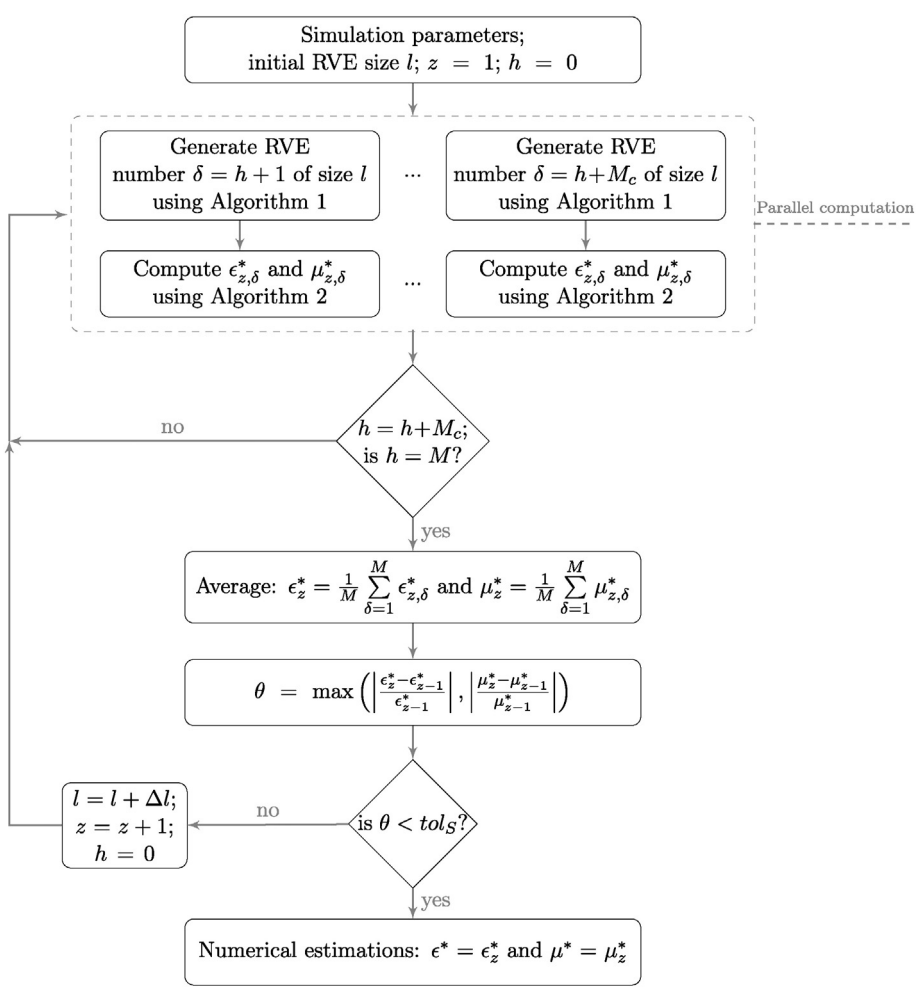

Fig. 6. Overall flowchart of the proposed numerical method to estimate the effective EM properties for a composite made with non-overlapping ellipsoidal particles.

Because Yee cell, a cubic grid, cannot capture exactly ellipsoidal particle shape, errors known as staircase errors [31] will be introduced at particle/matrix interface. To deal with this problem, we follow [9] and assume that there is no hard jump in properties in the actual composite but rather a smooth variation due to built up material at the interface that is a mix of matrix and particle material. This is taken into account numerically by using Laplacian property smoothing [9] at the interface, where any property P is replaced by a smooth spatial representation P^S as

$$P^S_{i,j,k} = \frac{1}{6}\left(P_{i+1,j,k} + P_{i-1,j,k} + P_{i,j+1,k} + P_{i,j-1,k} + P_{i,j,k+1} + P_{i,j,k-1}\right) \tag{19}$$

This omits the presence of hard jump in material properties at material interface, and remove the requirement to take into account for interface conditions. It is also important to mention that Yee's scheme converges to the actual solution only when the Courant–Friedrichs–Lewy (CFL) condition is met, which restricts the time step such that $\Delta t \leq \Delta t_{CFL} = \frac{1}{\sqrt{3}} \min_{s=1,3}(\Delta x_s) \min_{u=m,p}(\mu_u \epsilon_u)$. Finally, Yee's scheme requires the specification of boundary conditions for three of the six total components of **E** and **H** combined. In the present problem, the boundary conditions must satisfy certain criteria in order for the results computed over a RVE to be valid on the actual macroscale composite. This is derived by imposing energy conservation between the two scales as explained originally in [32] for mechanics, which is also extended to electromagnetism in [20]. It is shown that Dirichlet boundary conditions growing linearly in time satisfy this condition and are used here. We impose boundary conditions on the components of **E** by locating them on the outer side of the Yee cells on RVE boundary. Boundary values are increased up to a constant value at a slow linear rate in order to avoid the introduction of oscillating fields. Note that the magnitude of the boundary conditions should not influence the final estimation of the effective properties that are supposed to be constants of the composite. The fields are averaged numerically by summing over all nodes and dividing by the total number of nodes. Time stepping over a RVE is stopped once the variation of computed effective properties over two successive time step fall below a specified tolerance $tol_{\epsilon,\mu}$.

2.4. Overall description

An overall flowchart of the method is given in Fig. 6.

Algorithm 2. Computing effective EM properties over a RVE.

Input : RVE, Δt, Δx_s, properties $(\epsilon_m, \mu_m, \sigma_m)$ for matrix material, properties $(\epsilon_p^q, \mu_p^q, \sigma_p^q)$ for each particle of type q

Output: ϵ^* and μ^* for the given RVE

Divide RVE cube in Yee cells;
Associate properties $(\epsilon_u, \mu_u, \sigma_u)$ to grid node in phase u;
Do Laplacian smoothing of properties over the mesh;
Set initial and boundary conditions for **E** and **H**;
while $\max\left(\left|\frac{\epsilon^{*,n}-\epsilon^{*,n-1}}{\epsilon^{*,n-1}}\right|, \left|\frac{\mu^{*,n}-\mu^{*,n-1}}{\mu^{*,n-1}}\right|\right) \geq tol_{\epsilon,\mu}$ **do**
  $n = n + 1$; $t = t + \Delta t$;
  Update field **H** and **E** at each node (i, j, k) using equations 13 to 18 ;
  Compute field **D** and **B** using equations 11 and 12 ;
  Compute $\epsilon^{*,n}$ and $\mu^{*,n}$ from equations 3 and 4 respectively;
end

3. Applications and discussion

3.1. Validation with analytical bounds

The proposed numerical method has been implemented in Fortran language. It is first applied to problems where two-phase composites are considered. The numerical results are validated by verifying that they fall between the corresponding Hashin–Shtrikman bounds [11] — the tightest known bounds for effective electromagnetic properties of linear isotropic two-phase composites — that are expressed as

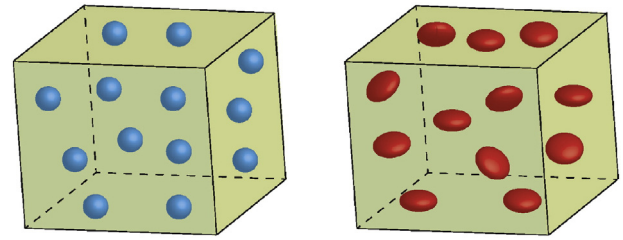

Fig. 7. Representation of RVEs with spherical and ellipsoidal particles.

$$P_1 + \frac{v_2}{\frac{1}{P_2 - P_1} + \frac{1 - v_2}{3P_1}} \leq P^* \leq P_2 + \frac{1 - v_2}{\frac{1}{P_1 - P_2} + \frac{v_2}{3P_2}} \tag{20}$$

where $P = \epsilon$ or μ, and for each property the subscript 2 refers to the material with the highest property value (in our examples it is the particles' property). We consider two types of microstructure, with one being the particular case of spherical particles. A sample RVE for each one is shown in Fig. 7. A list of all the parameters used is given in Table 1. Material properties are intentionally set close to obtain very narrow range for the bounds and validate the method properly (in an actual design, the composite would probably be made with polymer matrix with $\epsilon_{r,m}$ and $\mu_{r,m}$ close to 1, and dielectric or magnetic particles with $\epsilon_{r,p}$ and $\mu_{r,p}$ around 1000). Mesh refinement tests have been conducted before hand to estimate the required mesh size to ensure convergence of the numerically computed **E** and **H** fields in Yee's scheme. It was found that convergence occur for mesh size of around $\frac{\min(a_p, b_p, c_p)}{5}$. This value is thus used here. Evolution of relative effective electromagnetic properties for various volume fractions of particles v_p is presented in Fig. 8. We observe that numerical results successfully lie within the bounds defined by Hashin and Shtrikman.

To illustrate the validity of the method for composites made with several types of particles, it is also applied to a three-phase composite containing simultaneously the two types of particles used in the previous examples. A sample RVE is shown in Fig. 9. The best known bounds

Table 1
Simulation parameters for two-phase examples.

Parameters	Values
Relative electric permittivity $(\epsilon_{r,m}, \epsilon_{r,p})$	(1,10)
Relative magnetic permeability $(\mu_{r,m}, \mu_{r,p})$	(1,5)
Electric conductivity (σ_m, σ_p)	$(0,0)\ \frac{S}{m}$
Spherical particles radius r_p	$1\mu m$
Ellipsoidal particles semi axis (a_p, b_p, c_p)	$(0.8r_p, 0.9r_p, r_p)$
Initial RVE size $l = l_0$	$10r_p$
Size increment Δl	$0.1l_0$
Total number of RVE M	32
Simultaneous computation M_c	8
Tolerance on size variation tol_S	3%
Tolerance on properties variation $tol_{\mu,\epsilon}$	3%
Time step	$\Delta t = \Delta t_{CFL}$
Electric field E initial condition	$(0,0,0)\ \frac{V}{m}$
Electric field E boundary conditions	linearly growing up to $(1000,1000,1000)\ \frac{V}{m}$ from $t = 0$ to $t = 1000\Delta t$
Magnetic field H initial condition	$0\ A/m$ at $t = 0$

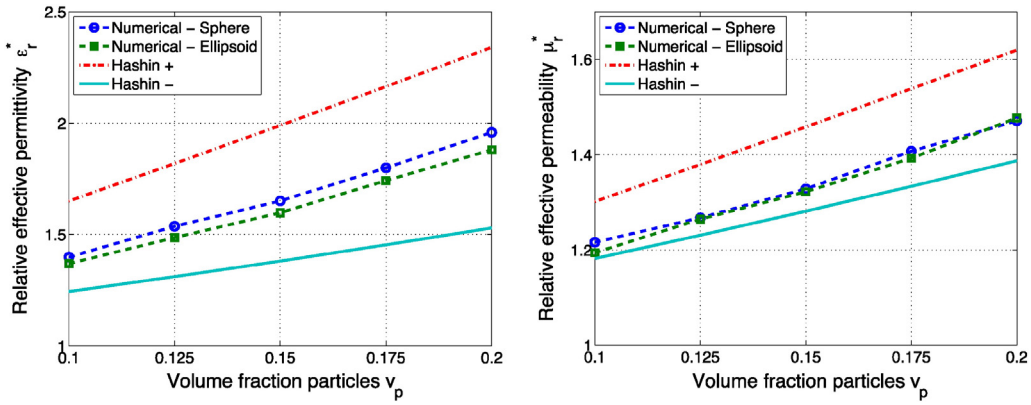

Fig. 8. Evolution of numerically estimated ε_r^* and μ_r^* for different volume fraction of particles, along with analytical Hashin and Shtrikman bounds.

for these types of microstructure are Wiener bounds [10], expressed as

$$\left(\frac{v_m}{P_m}+\frac{v_p^s}{P_p^s}+\frac{v_p^e}{P_p^e}\right)^{-1} \le P^* \le v_m P_m + v_p^s P_p^s + v_p^e P_p^e \tag{21}$$

where $P=\epsilon$ or μ, and superscripts s and e indicates properties of spherical and ellipsoidal particles, respectively. Material properties used are listed in Table 2, and all other parameters are chosen similar to the one listed in Table 1. The volume fraction of ellipsoidal particles is fixed to $v_p^e=0.05$. We show the evolution of relative effective electromagnetic properties for various volume fractions v_p^s of spherical particles in Fig. 10. The results again pass the analytical bounds test successfully.

3.2. Validation with experimental data

Finally, numerical results are compared to experimental data from [33] where the effective electric permittivity of a composite made by doping polyethylene (PE) with Barium Titanium ($BaTiO_3$) spherical particles is measured. The permittivity of matrix and particles as well as particles size are listed in [33]. The properties values not given in [33] were taken from various other sources. This is presented in Table 3. All other numerical parameters are chosen similar to the one listed in Table 1. Comparison between experimental and numerical results is shown in Fig. 11. We can observe that better estimation than analytical bounds is provided by the proposed method. However, differences with experimental data are noticeable, especially with increasing volume fraction. This could be due to several factors. Approximation of interface by smooth variation of properties rather than hard jump could reduce accuracy. The higher the volume fraction of particles, the higher is the number of interface, resulting in a higher overall error in effective properties estimation. This could be remedied by using alternate scheme for Maxwell's equations, able to capture more accurately particle geometry, such as the one described in [34] and [35]. Due to the complexity of these methods, we would however loose the simplicity and efficiency that motivated the choice of Yee's scheme. Moreover, it has been shown that interfacial layers that appear around particles for certain materials play an important role in macroscopic physical properties [36]. This is not taken into account in the numerical method and could lead to increasing error as particle volume fraction increases. Finally, external phenomena, such as temperature rise or material deformation, could play a significant role. However, they are not currently taken into account in the numerical modeling.

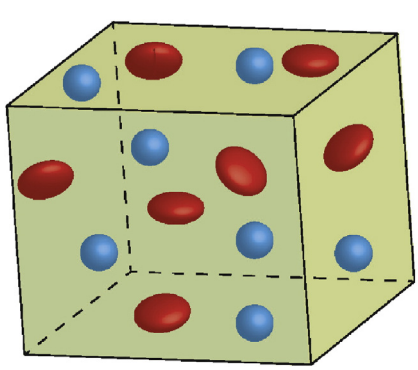

Fig. 9. Representation of a RVE with both spherical and ellipsoidal particles.

3.3. Benefits of parallelization

All the results shown previously were obtained on a single laptop with 2.6 GHz Intel Core i7 processor containing a total of 8 cores. All cores were used for best performance during computation of effective properties in the previous examples. To assess improvement provided by parallelization, we provide in Table 4 the central processing unit's (CPU) processing time required to compute effective properties using one core (no parallelization) to all 8 cores over 32 different RVEs of same size l_0 for the two-phase spherical particle composite case studied previously. We see that the computation time is significantly decreased with increasing the number of cores, justifying the parallel implementation.

4. Conclusions

Driven by the requirement to design particulate composites for electromagnetic applications, a numerical method to estimate the effective electromagnetic properties has been presented in this study. The overall method is designed to work with linear isotropic composites made with linear isotropic non-overlapping ellipsoidal particles. Multi-phase composites with several types of particles, varying in geometry and material nature, can be taken into account. Parallelization of a portion of the numerical solver has also been achieved decreasing the computational time significantly. The overall numerical implementation is realized such that the computation could be conducted on a single computer. The method has been tested on several composite microstructures, and the numerical results showed great agreement with the corresponding analytical bounds, ensuring validity of the method.

Table 2
Material properties used for three-phase composite simulation.

Material parameters	Values
Relative electric permittivity ($\epsilon_{r,m}, \epsilon_{r,p}^s, \epsilon_{r,p}^e$)	(1,10,7)
Relative magnetic permeability ($\mu_{r,m}, \mu_{r,p}^s, \mu_{r,p}^e$)	(1,5,2)
Electric conductivity ($\sigma_{r,m}, \sigma_{r,p}^s, \sigma_{r,p}^e$)	(0,0,0) S/m

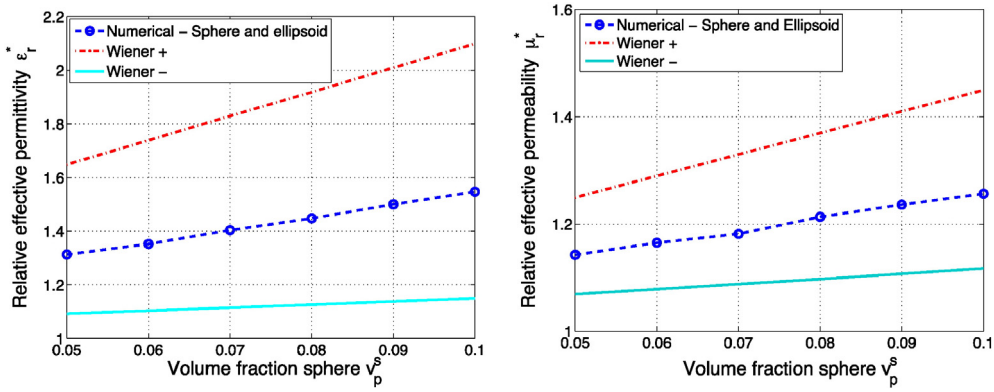

Fig. 10. Evolution of numerically estimated ε_r^* and μ_r^* for different volume fractions of spherical particles v_p^s, along with analytical Wiener bounds.

Table 3
Parameters used for validation with experimental data.

Parameters	Values
Relative electric permittivity ($\epsilon_{r,m}$,$\epsilon_{r,p}$) [33]	(1,72.5)
Relative magnetic permeability ($\mu_{r,m}$,$\mu_{r,p}$) [37]	(1.2,3)
Particle radius r_p [33]	$\approx 50\mu m$

Comparison with experimental data from literature showed more accurate results with the proposed method compared to the same analytical bounds.

This method is setting a basis upon which modifications could be realized to successively improve accuracy, expand to larger type of composites, and consider effect of external physical phenomena, in order to build the ideal design tool. An alternate scheme for Maxwell's equations, able to capture more accurately particle geometry can be implemented to potentially improve the accuracy of the results, especially at higher volume fraction. Factors such as temperature variation or interfacial layer at particles surface have been shown to influence the effective properties significantly, and taking them into account would further improve accuracy of the numerical estimations. Because dynamic Maxwell's equations have been considered here, these dynamic phenomena could be taken into account simply by adding relevant governing equations along with adequate numerical method to solve them. Extension of the method to larger type of composite could be realized. For instance, particle shape other than ellipsoidal could be considered by incorporating adequate RVE generating and non-overlapping

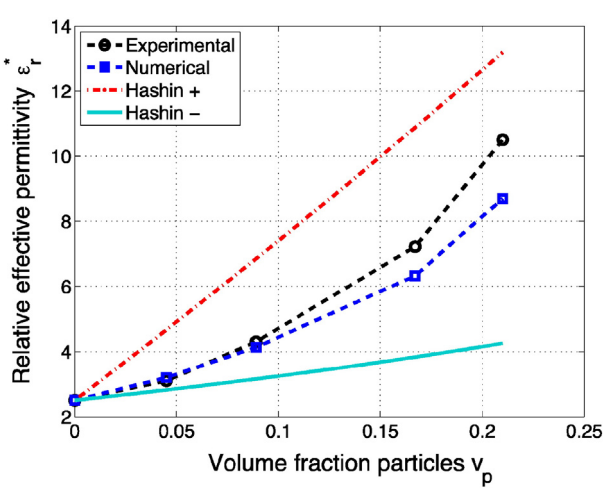

Fig. 11. Evolution of the numerically estimated effective electric permittivity ε_r^* along with analytical bounds and experimental results from [33].

Table 4
CPU time required to compute effective electromagnetic properties over 32 different RVEs of same size.

Number of cores used	CPU time (s)	Time reduction compared to non-parallelized computation (%)
1	5438	0
2	2801	48
4	2132	61
8	1685	69

check methods. Moreover, adaption to anisotropic materials could be envisioned by considering properties to be represented as tensor quantities instead of scalars. Each effective property would then have nine unknowns that could be estimated using nine independent numerical tests similar to the one described in this work. Finally, combination of this method with an optimization technique, to determine optimal parameters for a composite to achieve desired effective EM properties, would provide a complete design tool. This is all currently under consideration by the authors.

Acknowledgments

The authors gratefully acknowledge the financial support of King Abdullah University of Science and Technology (KAUST) during this research. The authors also thank Aashish Ahuja, Zeyad Zaky, and Rishi Ganeriwala for their assistance in the revision of the paper.

References

[1] R. Ghodssi, P. Lin, MEMS Materials and Processes Handbook, vol. 1Springer, 2011.
[2] D.D. Chung, Composite Materials: Functional Materials for Modern Technologies, Springer Science & Business Media, 2003.
[3] X. Chou, Z. Zhao, W. Zhang, J. Zhai, Microstructures and dielectric properties of ba 0.5 sr 0.5 tio 3–zn 2 tio 4 composite ceramics with low sintering temperature for tunable device applications, Mater. Des. 31 (8) (2010) 3703–3707.
[4] I. Bishay, S. Abd-El-Messieh, S. Mansour, Electrical, mechanical and thermal properties of polyvinyl chloride composites filled with aluminum powder, Mater. Des. 32 (1) (2011) 62–68.
[5] J.C. Toor, A. Cheng, A.P. Pisano, Synthesis and Characterization of Gold Nanoparticle/Su-8 Polymer Based Nanocomposite, 2014.
[6] T. Siponkoski, M. Nelo, J. Peräntie, J. Juuti, H. Jantunen, Batio 3–p (vdf-trfe) composite ink properties for printed decoupling capacitors, Compos. Part B 70 (2015) 201–205.
[7] K. Koh, J. Park, J. Park, X. Zhu, L. Lin, Core-shell magnetic nanoparticles for on-chip rf inductors, in: Micro Electro Mechanical Systems (MEMS), 2013 IEEE 26th International Conference on, IEEE 2013, pp. 465–468.
[8] S. Torquato, Random Heterogeneous Materials: Microstructure and Macroscopic Properties, vol. 16Springer Science & Business Media, 2002.
[9] T. Zohdi, Simulation of coupled microscale multiphysical-fields in particulate-doped dielectrics with staggered adaptive fdtd, Comput. Methods Appl. Mech. Eng. 199 (49) (2010) 3250–3269.
[10] O. Wiener, Zur theorie der refraktionskonstanten. berichte uber die verhandlungen der koniglich-sachsischen gesellschaft der wissenshaften zu leipzig, Math.–Phys. Klasses 62 (1910) 256–277.

[11] Z. Hashin, S. Shtrikman, A variational approach to the theory of the effective magnetic permeability of multiphase materials, J. Appl. Phys. 33 (10) (1962) 3125–3131.
[12] J.M. Garnett, Colours in metal glasses, in metallic films, and in metallic solutions. II, Philosophical Transactions of the Royal Society of London. Series A, Containing Papers of a Mathematical or Physical Character 1906, pp. 237–288.
[13] J. Aboudi, Mechanics of Composite Materials: A Unified Micromechanical Approach, Elsevier, 2013.
[14] T.I. Zohdi, P. Wriggers, An Introduction to Computational Micromechanics, Springer Science & Business Media, 2008.
[15] J.C. Maxwell, A Treatise on Electricity and Magnetism, Vol. 1, Clarendon press, 1881.
[16] K.S. Yee, Numerical solution of initial boundary value problems involving Maxwell's equations, IEEE Trans. Antennas Propag. 14 (3) (1966) 302–307.
[17] A. Nigrawal, N. Chand, Development and electrical characterization of carbon soot filled polyester graded composites, Mater. Des. 31 (8) (2010) 3672–3676.
[18] D.B. Sirdeshmukh, L. Sirdeshmukh, K. Subhadra, Micro-and Macro-properties of Solids, Springer, 2006.
[19] S. Somiya, Handbook of Advanced Ceramics: Materials, Applications, Processing, and Properties, Academic Press, 2013.
[20] T.I. Zohdi, Electromagnetic Properties of Multiphase Dielectrics: A Primer on Modeling, Theory and Computation, vol. 64Springer Science & Business Media, 2012.
[21] K. Sab, On the homogenization and the simulation of random materials, Eur. J. Mech. A. Solids 11 (5) (1992) 585–607.
[22] W. Drugan, J. Willis, A micromechanics-based nonlocal constitutive equation and estimates of representative volume element size for elastic composites, J. Mech. Phys. Solids 44 (4) (1996) 497–524.
[23] L. Bouhala, Y. Koutsawa, A. Makradi, S. Belouettar, An advanced numerical method for predicting effective elastic properties of heterogeneous composite materials, Compos. Struct. 117 (2014) 114–123.
[24] S. Alfano, M.L. Greer, Determining if two solid ellipsoids intersect, J. Guid. Control. Dyn. 26 (1) (2003) 106–110.
[25] W. Tian, L. Qi, J. Zhou, J. Liang, Y. Ma, Representative volume element for composites reinforced by spatially randomly distributed discontinuous fibers and its applications, Compos. Struct. 44 (2015) 366–373.
[26] J.D. Jackson, Classical Electrodynamics, third ed. Wiley, 1998.
[27] A. Kovetz, Electromagnetic Theory, Oxford University Press Oxford, 2000.
[28] D.J. Griffiths, Introduction to Electrodynamics, Pearson, 2013.
[29] A. Taflove, S.C. Hagness, Computational Electrodynamics, 160, Artech house Boston, 2000.
[30] T. Rylander, P. Ingelström, A. Bondeson, Computational Electromagnetics, 51, Springer Science & Business Media, 2012.
[31] J. Häggblad, O. Runborg, Accuracy of staircase approximations in finite-difference methods for wave propagation, Numer. Math. 128 (4) (2014) 741–771.
[32] R. Hill, The elastic behaviour of a crystalline aggregate, Proc. Phys. Soc. London Sect. A 65 (5) (1952) 349.
[33] M. Takeuchi, An experimental study on the effective dielectric constant of heterogeneous media, Properties and Applications of Dielectric Materials, 1991., Proceedings of the 3rd International Conference on, IEEE 1991, pp. 1064–1067.
[34] K. Dridi, J.S. Hesthaven, A. Ditkowski, Staircase-free finite-difference time-domain formulation for general materials in complex geometries, Antennas Propag. IEEE Trans. 49 (5) (2001) 749–756.
[35] J. Anderson, M. Okoniewski, S. Stuchly, Practical 3-d contour/staircase treatment of metals in fdtd, Microw. Guided Wave Lett. IEEE 6 (3) (1996) 146–148.
[36] W. Xu, H. Chen, W. Chen, L. Jiang, Prediction of transport behaviors of particulate composites considering microstructures of soft interfacial layers around ellipsoidal aggregate particles, Soft Matter 10 (4) (2014) 627–638.
[37] G.W.C. Kaye, T.H. Laby, Tables of Physical and Chemical Constants and Some Mathematical Functions, Longmans, Green and Company, 1921.